

The Influence of Phosphane Coligands on the Nuclearity of Rhodium(I) 4-Thiolatobenzoic Acid Complexes

Ulrike Helmstedt, Peter Lönnecke,[†] and Evamarie Hey-Hawkins*

Institut für Anorganische Chemie der Universität Leipzig, Johannisallee 29,
D-04103 Leipzig, Germany

Received June 14, 2006

[RhCl(PR₃)₃] (R = Ph, Et) reacts with the potassium salt of 4-mercaptobenzoic acid to give a mixture of the monomeric and dimeric complexes, [Rh(SC₆H₄COOH)(PR₃)₃] and [Rh(μ-SC₆H₄COOH)(PR₃)₂]₂, respectively. With the labile PPh₃ coligand, the dimer is the major product, while for the electron-rich coligand PEt₃, the equilibrium is easily shifted to the monomer by the addition of excess PEt₃. Phosphane dissociation and dimerization could be prevented by using the chelating coligand PPh(C₂H₄PPh₂)₂. [Rh(μ-SC₆H₄COOH)(PPh(C₂H₄PPh₂)₂)]₂ (**2b**), [Rh(SC₆H₄COOH)(PEt₃)₃] (**3a**), and [Rh(SC₆H₄COOH){PPh(C₂H₄PPh₂)₂}] (**4**) were fully characterized by nuclear magnetic resonance and infrared spectroscopy, mass spectrometry, and elemental analysis. The molecular structures of **2b** and **4** were determined by X-ray structure analysis. In solution, the lability of the phosphane ligands leads to the decomposition of **2b**. One of the decomposition products, namely, the mixed-valent complex [Rh^IRh^{III}(μ-SC₆H₄COO)(μ-SC₆H₄COOH)(SC₆H₄COOH)(PPh₃)₃]₂ (**5**), was characterized by X-ray structural analysis. The dinuclear rhodium(III) complex [Rh(μ-SC₆H₄COO)(SC₆H₄COOH)(PEt₃)₂]₂ (**6**) was shown to be a byproduct in the synthesis of **3a**, and this demonstrates the reactivity of the rhodium(I) complexes toward oxidative addition. The structurally characterized complexes **2b**, **4**, **5**, and **6** show hydrogen bonding of the free carboxyl groups.

Introduction

Transition-metal complexes with thiolato ligands have attracted increasing attention in view of their role in the desulfurization of organosulfur compounds,¹ especially the hydrodesulfurization of fossil fuel feedstocks,² metal-catalyzed C–S bond cleavage and formation in organic synthesis,³ and in the degradation of the thiolato ligands to yield transition-metal sulfides.⁴ Some of these reactions involve rhodium(I) thiolato phosphane complexes as intermediates. Stable mononuclear rhodium(I) complexes of the

type [Rh(SR)(PR'₃)₃] with tertiary phosphane ligands are especially of interest, because they apparently show higher reactivity toward electrophiles than the well-investigated dinuclear thiolato-bridged complexes.⁵ To date, only a limited number of stable monomeric rhodium(I) thiolato complexes is known, that is, [Rh(SC₆F₅)(PR₃)₃] for PR₃ = PPh₃, PMePh₂, PMe₂Ph, P(OMe)₃, and P(OEt)₃⁶ and [Rh(SR)-(PMe₃)₃] for SR = SC₆H₅, 4-SC₆H₄Me, and 4-SC₆H₄OMe.⁷ Other known phosphane complexes of rhodium(I) thiolates eliminate one phosphane ligand per rhodium center at room

* To whom correspondence should be addressed. Tel.: +49-(0)341-9736151. Fax: +49-(0)341-9739319. E-mail: hey@rz.uni-leipzig.de.

[†] Crystal structure determinations.

- (1) (a) Kwart, H.; Schuit, G. C. A.; Gates, B. C. *J. Catal.* **1980**, *61*, 128. (b) Zaera, F.; Kollin, E. B.; Gland, J. L. *Surf. Sci.* **1987**, *184*, 75. (c) Eisch, J. J.; Hallenbeck, L. E.; Han, K. I. *J. Org. Chem.* **1983**, *48*, 2963. (d) Rauchfuss, T. B. *Prog. Inorg. Chem.* **1991**, *39*, 259.
- (2) (a) Bianchini, C.; Casares, J. A.; Meli, A.; Sernau, V.; Vizza, F.; Sánchez-Delgado, R. A. *Polyhedron* **1997**, *16*, 3099. (b) Bianchini, C.; Herrera, V.; Jimenez, M. V.; Meli, A.; Sánchez-Delgado, R. A.; Vizza, F. *J. Am. Chem. Soc.* **1995**, *117*, 8567.
- (3) (a) Okamura, H.; Miura, M.; Takei, H. *Tetrahedron Lett.* **1979**, *43*. (b) Wenkert, E.; Ferreira, T. W.; Michelotti, E. L. *J. Chem. Soc., Chem. Commun.* **1979**, 637. (c) Wenkert, E.; Hanna, J. M.; Leftin, M. H.; Michelotti, E. L.; Potts, K. T. *J. Org. Chem.* **1985**, *50*, 1125.

- (4) (a) Osakada, K.; Yamamoto, T. *Inorg. Chem.* **1991**, *30*, 2328. (b) Bochmann, M.; Hawkins, I.; Wilson, L. M. *J. Chem. Soc., Chem. Commun.* **1988**, 344. (c) Brennan, J. G.; Siegrist, T.; Carroll, R. J.; Stuczynski, S. M.; Brus, L. E.; Steigerwald, M. E. *J. Am. Chem. Soc.* **1989**, *111*, 4141. (d) Nomura, R.; Fujii, S.; Kanaya, K.; Matsuda, H. *Polyhedron* **1990**, *9*, 361.
- (5) (a) Carlton, L.; Bulbulia, Z. *J. Organomet. Chem.* **1990**, *389*, 139. (b) Bonnet, J. J.; Kalck, P.; Poilblanc, R. *Inorg. Chem.* **1977**, *16*, 1514. (c) Cruz-Garriz, D.; Garcia-Allejandro, J.; Torrens, H.; Alvarez, C.; Toscano, R. A.; Poilblanc, R.; Thorez, A. *Transition Met. Chem.* **1991**, *16*, 130.
- (6) (a) Beck, W.; Tadros, S. Z. *Anorg. Allg. Chem.* **1970**, *375*, 231. (b) Carlton, L. *J. Organomet. Chem.* **1992**, *431*, 103.
- (7) (a) Osakada, K.; Hataya, K.; Yamamoto, T. *Inorg. Chem.* **1993**, *32*, 2360. (b) Osakada, K.; Hataya, K.; Yamamoto, T. *Organometallics* **1993**, *12*, 3358.

temperature and dimerize with the formation of $[\{\text{Rh}(\mu\text{-SR})(\text{PR}'_3)_2\}_2]$.^{5a,8} The tendency to dimerize decreases with decreasing electron density of the thiolato ligand and with increasing electron density of the phosphane ligands. Known syntheses include the oxidative addition of thiols RSH to $[\text{RhH}(\text{PPh}_3)_4]$ followed by H_2 elimination,^{5a,9} salt elimination reactions of $[\text{RhCl}(\text{PR}_3)_3]$ and alkali-metal thiolates,^{6a,7} and the reaction of the dimeric complexes with excess phosphane.¹⁰

We are interested in heterometallic complexes,¹¹ the synthetic approach being the synthesis of mononuclear monometallic complexes of bifunctional ligands, which are then coordinated to the second metal center to form the heterometallic species. Interest in early/late heterobimetallics has strongly increased in the past few decades.¹² The reasons for this are mainly the explanation of the strong metal–support interaction phenomenon in heterogeneous catalysis¹³ and the applicability of cooperative effects between different metal centers for catalysts¹⁴ and magnetic materials.¹⁵ Of special interest for these applications is the investigation of metal–metal interactions. These can be achieved either by direct contact of the metal centers in the compounds¹⁶ or with the help of bridging ligands which allow electronic interactions via π -conjugated bridges.¹⁷ Therefore, rhodium(I) complexes of the type $[\text{Rh}(\text{SR})(\text{PR}'_3)_3]$, where SR is a thiolato ligand which contains a second donor group in a conjugated backbone, are intriguing metalloligands for the synthesis of heterometallic complexes. We therefore investigated the preparation and characterization of rhodium(I) complexes with the anion of 4-mercaptobenzoic acid as a ligand. We present here a study of the influence of the phosphane coligands on the tendency of the products $[\text{Rh}(\text{SC}_6\text{H}_4\text{CO}_2\text{H})(\text{PR}_3)_3]$ to dimerize. Furthermore, the tendency of these complexes to undergo oxidative addition is exemplified by the formation of the mixed-valent complex $[\{\text{Rh}^{\text{I}}\text{Rh}^{\text{III}}(\mu\text{-SC}_6\text{H}_4\text{COO})(\mu\text{-SC}_6\text{H}_4\text{COOH})(\text{SC}_6\text{H}_4\text{COOH})(\text{PPh}_3)_3\}_2]$ (**5**) and the dinuclear rhodium(III) complex $[\{\text{Rh}(\mu\text{-SC}_6\text{H}_4\text{COO})(\text{SC}_6\text{H}_4\text{COOH})(\text{PEt}_3)_2\}_2]$ (**6**). The structurally characterized complexes **2b**, **4**, **5**, and **6** exhibit interesting structures in the solid state, due to the ability of free carboxyl groups to associate by hydrogen bonding.

Experimental Section

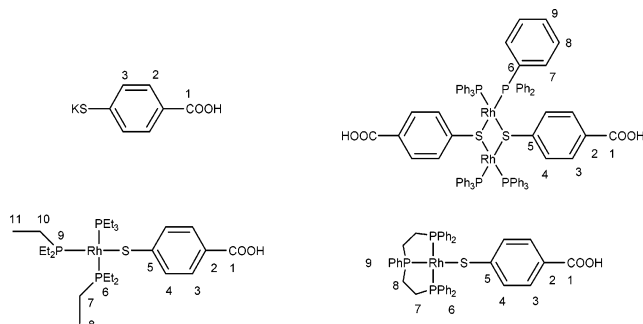
General Remarks. All experiments were carried out under purified dry nitrogen. Solvents were dried and freshly distilled under nitrogen. The nuclear magnetic resonance (NMR) spectra were recorded at 25 °C with a Bruker AVANCE DRX 400 spectrometer (^1H NMR 400.13 MHz, ^{13}C NMR 100.3 MHz, ^{31}P NMR 161.97 MHz); $\text{Si}(\text{CH}_3)_4$ was used as the internal standard in the ^1H NMR spectra. Coupling constants for the AA'BB' systems of the mba fragment could not be obtained by simulation because of a high line width, which probably occurs due to hindered rotation. All heteronuclei spectra were referenced to $\text{Si}(\text{CH}_3)_4$ with the Ξ scale.¹⁸ ^{31}P MAS NMR (202.45 MHz) were performed with a Bruker MSL 500 spectrometer. The IR spectra were recorded on a Fourier transform infrared spectrometer Perkin-Elmer Spektrum 2000 (KBr) in the range 350–4000 cm^{-1} . The mass spectra were recorded with a VG ZAB-HSQ [fast atom bombardment (FAB), 3-nitrobenzyl alcohol matrix] or with a Fourier transform ion cyclotron resonance mass spectrometer, type APEX II (Bruker-Daltonics). Elemental composition was determined with a Hereaus CHN–O–S analyzer. The melting points were determined in sealed capillaries under nitrogen using a Gallenkamp apparatus and are uncorrected. 4-Mercaptobenzoic acid (H_2mba) is commercially available and was used as received. $[\text{RhCl}(\text{PPh}_3)_3]$,¹⁹ $[\text{RhCl}(\text{PEt}_3)_3]$,²⁰ and $[\text{RhCl}\{\text{PPh}(\text{C}_2\text{H}_4\text{PPh}_2)_2\}_2]$ ²¹ were prepared according to literature procedures.

K(Hmba) (1). A solution of KO^tBu (1.5 g, 13.4 mmol) in tetrahydrofuran (THF; 20 mL) was added over 1 h to a solution of H_2mba (2.1 g, 13.6 mmol) in THF (60 mL) at room temperature. The resulting colorless suspension was stirred for 30 min. The product was isolated by filtration, washed with THF (3 × 10 mL), and dried in vacuo (yield: 1.75 g, 67%). K(Hmba) (**1**) is soluble in water and slightly soluble in dimethylsulfoxide (DMSO). Elem. anal. calcd (%) for $\text{C}_7\text{H}_5\text{KO}_2\text{S}$ ($M = 192.28$): C, 43.72; H, 2.62. Found: C, 43.39; H, 2.82. ^1H NMR (DMSO- d_6): δ 7.02 (d, 2H, $^3J_{\text{HH}} = 8.0$ Hz, H2), 7.22 (d, 2H, $^3J_{\text{HH}} = 8.0$ Hz, H3), 11.6 ppm (s, br, 1H, H1). IR (KBr): $\tilde{\nu}$ 3061 w, 2522 w, 1655 w, 1586 s, 1542 s, 1400 s, 1180 m, 1100 s, 915 w, 855 w, 840 m, 770 s, 725 w, 689 w, 519 m, 474 m cm^{-1} . ESI-MS (high res., neg.) found: m/z 724.8628 $\{[\text{K}_3(\text{mba})_4]^{-}, 11.7\%$, 686.9087 $\{[\text{K}_2\text{H}(\text{mba})_4]^{-}, 21.4\%$, 648.9522 $\{[\text{KH}_2(\text{mba})_4]^{-}, 16.5\%$, 610.9970 $\{[\text{H}_3(\text{mba})_4]^{-}, 34.0\%$, 342.9508 $\{[\text{K}(\text{mba})_2]^{-}, 21.0\%$, 304.9952 $\{[\text{H}(\text{mba})_2]^{-}, 100\%$. The calculated isotopic patterns are in agreement with the observed ones.

Di- μ (S)-(4-carboxybenzenethiolato)-bis{di(triphenylphosphane)}dirhodium(I), $[\{\text{Rh}(\mu\text{-SC}_6\text{H}_4\text{COOH})(\text{PPh}_3)_2\}_2]$ (2b**).** A solution of $[\text{RhCl}(\text{PPh}_3)_3]$ (390 mg, 0.42 mmol) in THF (80 mL) was added via cannula to a suspension of K(Hmba) (81 mg, 0.42 mmol) in THF (70 mL). The suspension was heated to 50 °C for 4 h. The resulting orange solution was separated from the solid by filtration and the volume reduced to ca. 5 mL. At room temperature, the product was obtained as orange crystals (157 mg), isolated, washed with cold THF and *n*-hexane, and dried in vacuo. Concentrating the mother liquor gave another crop of crystals (100 mg), which had to be recrystallized from THF to remove PPh_3 . The product was obtained as orange blocks (yield: 239 mg, 73%)

- (8) (a) Carlton, L. *Magn. Reson. Chem.* **1997**, *35*, 153. (b) Osakada, K.; Matsumoto, K.; Yamamoto, T.; Yamamoto, A. *Organometallics* **1985**, *4*, 857.
 (9) Osakada, K.; Yamamoto, T. *Bull. Chem. Soc. Jpn.* **1994**, *67*, 3271.
 (10) Carlton, L. *J. Organomet. Chem.* **1992**, *431*, 103.
 (11) Helmstedt, U.; Lönnecke, P.; Reinhold, J.; Hey-Hawkins, E. *Eur. J. Inorg. Chem.* In press.
 (12) Stephan, D. W. *Coord. Chem. Rev.* **1989**, *95*, 41.
 (13) Tauster, S. J. *Acc. Chem. Res.* **1978**, *20*, 389.
 (14) (a) Rida, M. A.; Smith, A. K. In *Modern Coordination Chemistry—A Legacy to J. Chatt*; Leigh, J. J., Winterton, N., Ed.; RSC: London, 2002; pp 154–161. (b) Senocq, F.; Randrianalimanana, C.; Thorez, A.; Kalck, P.; Choukroun, R.; Gervais, D. *J. Chem. Soc., Chem. Commun.* **1984**, 1376. (c) Choukroun, R.; Gervais, D.; Jaud, J.; Kalck, P.; Senocq, F. *J. Organomet. Chem.* **1986**, *5*, 67. (d) Partenheimer, W. Amoco Corp. U.S. Patent 4,992,580, DATE.
 (15) Kahn, O. *Adv. Inorg. Chem.* **1995**, *43*, 179.
 (16) Bullock, R. M.; Casey, C. P. *Acc. Chem. Res.* **1987**, *20*, 167.
 (17) (a) Back, S.; Stein, T.; Frosch, W.; Wu, I.; Kralik, J.; Büchner, M.; Huttner, G.; Rheinwald, G.; Lang, H. *Inorg. Chim. Acta* **2001**, *325*, 94. (b) Plenio, H.; Burth, D. *Organometallics* **1996**, *15*, 4054.

- (18) Harris, R. H.; Becher, E. D.; Cabral de Menezes, S. M.; Goodfellow, R.; Granger, P. *Concepts Magn. Reson.* **2002**, *14*, 326.
 (19) Osborn, J. A.; Jardine, F. H.; Young, J. F.; Wilkinson, G. *J. Chem. Soc. A* **1966**, 1711.
 (20) Intille, G. M. *Inorg. Chem.* **1972**, *11*, 695.
 (21) (a) Nappier, T. E.; Meek, D. W. *J. Am. Chem. Soc.* **1972**, *94*, 306. (b) Westcott, S. A.; Stringer, G.; Anderson, S.; Taylor, N. J.; Marder, T. B. *Inorg. Chem.* **1994**, *33*, 4589. (c) King, R. B.; Kapoor, P. N.; Kapoor, R. N. *Inorg. Chem.* **1971**, *10*, 1841.

Scheme 1. Numbering Scheme for the Assignment of the Signals in the NMR Spectra

and is soluble in THF. Compound **2b** is air-stable for several weeks as a solid but air- and moisture-sensitive in solution. Melting point: 220 °C (decomp.). Elem. anal. calcd (%) for $C_{86}H_{70}O_4P_4Rh_2S_2$ ($M_m = 1561.31$): C, 66.21; H, 4.58. Found: C, 66.04; H, 4.48. Compound **2** slowly decomposes in solution; therefore, the NMR spectra could only be obtained in the presence of 1 equiv of PPh_3 to stabilize **2b** in solution. Only signals of **2b** are given (see Scheme 1 for the numbering scheme assignments of the signals in the NMR spectra). 1H NMR (THF- d_8): δ 6.68 (m, 4H, A part of the AA'BB' spin system, H4), 6.77 (d, 4H, B part of the AA'BB' spin system, H3), 6.92 (m, 24H, H7), 7.04 (t, 12H, $^3J_{HH} = 7.6$ Hz, H9), 7.54 ppm (m, 24H, H8), OH not observed. $^{13}C\{^1H\}$ NMR (THF- d_8): δ 126.4 (s, C4), 126.7 (m, C7) † , 127.9 (s, C9), 128.0 (s, C5), 131.8 (m, C6) † , 134.4 (s, C3), 134.6 (m, C8) † , 151.6 (s, C2), 172.7 ppm (s, C1) († coupling constants J_{A-X} , $J_{A'-X}$, and J_{M-X} could not be obtained by simulation because of a high line width and low signal-to-noise ratio). $^{31}P\{^1H\}$ NMR (THF- d_8): δ 41.9 ppm (d, $^1J_{RhP} = 168.9$ Hz, PPh_3). IR (KBr): $\tilde{\nu}$ 3052 m, 2960 w, 1682 s, 1586 s, 1552 m, 1480 m, 1434 s, 1416 s, 1305 s, 1171 m, 1120 m, 1091 s, 1027 m, 1016 m, 846 m, 805 m, 741 s, 722 m, 694 s, 534 s, 521 s, 493 m, 432 cm^{-1} . FAB-MS found (pos.): m/z 766.1 {[Rh(SC₆H₄COH)(PPh₃)₂ + 2H] $^+$, 0.4%}, 627.1 {[Rh-(PPh₃)₂] $^+$, 1%}, 613.1 {[Rh(SC₆H₄COH)(PPh₃)₂ - 2Ph + 2H] $^+$, 2%}, 154.0 {[HOCC₆H₄SH] $^+$, 95%}, 136.0 {[OCC₆H₄S + 2H] $^+$, 100%}. The calculated isotopic patterns are in agreement with the observed ones.

4-Carboxybenzenethiolato-tris(triethylphosphane)-rhodium(I), [Rh(SC₆H₄COOH)(PEt₃)₃] (3a). A solution of [RhCl(PEt₃)₃] (162 mg, 0.33 mmol) and PEt₃ (1 mL) in THF (7 mL) was added to a suspension of K(Hmba) (67 mg, 0.35 mmol) in THF (7 mL) at 0 °C. The suspension was allowed to warm to room temperature and was stirred for 16 h. The red solution was filtered [this was performed under argon, as the filtration takes about 8 h (very fine solid) and the product is very air-sensitive], and the solvent was removed in vacuo. The dark orange solid was washed with cold THF (1 mL) and *n*-hexane (2 × 5 mL) and dried in vacuo (yield: 147 mg, 73%). Compound **3a** is soluble in THF and slightly soluble in toluene. At room temperature, an orange solid precipitates from solution, which is almost insoluble in all common solvents, but shows the same elemental analyses and IR spectroscopic data as **3a**. Melting point: 201–205 °C (decomp.). Elem. anal. calcd (%) for $C_{25}H_{50}O_2P_3RhS$ ($M = 610.56$): C, 49.18; H, 8.25. Found: C, 49.11; H, 8.18. For the stabilization of **3a** in solution, 10 equiv of PEt₃ were added to the NMR tube. Only the signals of **3a** are given. 1H NMR (THF- d_8): δ 1.00–1.90 (m, 45H, PEt₃), 7.48 (m, 2H, A part of the AA'BB' spin system, H4), 7.90 ppm (m, 2H, B part of the AA'BB' spin system, H3), OH not observed. $^{13}C\{^1H\}$ NMR (THF- d_8): δ 8.3 (C8), 8.7 (C11), 17.3 (C7), 21.3 (C10), 122.3 (C5), 127.3 (2s, C4), 131.1 (C3), 162.4 (C2), 163.0 ppm (C1). $^{31}P\{^1H\}$ NMR (THF- d_8): δ 12.1 (dd, $^1J_{RhP} = 136.4$ Hz, $^2J_{PP} =$

38.6 Hz, P6), 26.7 (dt, $^1J_{RhP} = 161.8$ Hz, $^2J_{PP} = 38.3$ Hz, P9). IR (KBr): $\tilde{\nu}$ 3059 w, 2962 s, 2935 s (sh), 2877 m, 2649 w, 2544 w (sh), 1663 s, 1579 s (sh), 1533 m, 1457 m, 1415 s, 1376 m, 1301 m (sh), 1284 s (sh), 1166 m, 1126 m, 1084 s, 1031 s, 999 m, 863 w, 844 w, 805 w, 766 s, 729 m, 704 m, 672 w, 655 w, 616 w, 550 w, 531 w, 477 w, 431 w, 412 cm^{-1} . FAB-MS found (pos.): m/z 593.0 {[Rh(SC₆H₄COOH)(PEt₃)₃ - H₂O + H] $^+$, 10%}, 567.0 {[Rh(SC₆H₄COOH)(PEt₃)₃ - CO₂ + H] $^+$, 7.7%}, 565.0 {[Rh(SC₆H₄COOH)(PEt₃)₃ - CO - H₂O + H] $^+$, 9.0%}.

4-Carboxybenzenethiolato-bis(diphenylphosphanylene)-phenylphosphane-rhodium(I), [Rh(SC₆H₄COOH){PPh(C₂H₄PPh₂)₂}] (4). A solution of H₂miba (76 mg, 0.49 mmol) in THF (30 mL) was added over 30 min to a solution of [RhCl{PPh(C₂H₄PPh₂)₂}] (330 mg, 0.49 mmol) and N^tBu_3 (0.15 mL, 0.49 mmol) in THF (60 mL) at room temperature. The color changed from bright yellow to pale brown. The solution was stirred overnight. The solvent was removed in vacuo, and the ochre residue was washed with toluene (2 × 2.5 mL) and *n*-hexane (5 mL), dissolved in THF (20 mL), and precipitated by the addition of *n*-hexane (50 mL). The yellow solid was dried in vacuo (yield: 368 mg, 95%). Compound **4** is highly air- and moisture-sensitive. Single crystals suitable for X-ray analysis were obtained by layering a concentrated solution of **4** in THF with twice the volume of *n*-hexane. Pure **4** is almost insoluble in common organic solvents (*n*-hexane, toluene, benzene, THF, CH₃CN, and DMSO) and dissolves in *N,N*-dimethylformamide (DMF) with decomposition. Melting point: 205–208 °C (decomp.). Elem. anal. calcd (%) for $C_{41}H_{38}O_2P_3RhS$ ($M = 790.63$): C, 62.28; H, 4.84. Found: C, 62.31; H, 4.76. Because of the low solubility of pure **4**, 1H and ^{31}P NMR spectroscopic characterizations were carried out with the solid containing traces of impurities (grease, solvent, and N^tBu_3). Only the signals of **4** are given. 1H NMR (THF- d_8): δ 1.6–1.8 (2m, 4H, H8), 2.5–2.9 (3m, 4H, H7), 7.07–8.08 ppm (m, 29H, H3, H4, H6, H9), OH not observed. $^{31}P\{^1H\}$ NMR (THF- d_8): δ 47.6 (dd, $^1J_{RhP} = 150.9$ Hz, $^2J_{PP} = 32.0$ Hz, P6), 106.9 (dt, $^1J_{RhP} = 138.2$ Hz, $^2J_{PP} = 31.9$ Hz, P9). IR (KBr): $\tilde{\nu}$ 3051 m, 2958 w (sh), 1671 m (sh), 1580 s, 1482 w, 1435 s, 1411 m, 1306 w, 1265 w, 1168 m, 1098 s (sh), 1027 m, 890 w, 866 w, 808 w, 744 m, 696 s, 518 m, 485 cm^{-1} . FAB-MS found (pos.): m/z 789.1 ([M - H] $^+$, 51%), 672.1 ([Rh(SH){PPh(C₂H₄PPh₂)₂} + 2H] $^+$, 22%), 637.1 ([Rh{PPh(C₂H₄PPh₂)₂}] $^+$, 72%). The calculated isotopic patterns are in agreement with the observed ones.

Data Collection and Structure Determination. X-ray data (Table 1) were collected with a Siemens CCD-Smart diffractometer for **4** and with a Stoe IPDS1 for **2b**, **5**, and **6** using graphite-monochromated Mo K α radiation ($\lambda = 0.71073$ Å). Absorption correction was performed with the program SADABS²² for **4** and numerically for **2b**, **5**, and **6**. Structure solution and refinement were performed with WinGX,²³ SHELXS-97, and SHELXL-97.²⁴ All non-hydrogen atoms were refined anisotropically; most hydrogen atoms were refined in calculated positions. Visualization was carried out with the program DIAMOND. CCDC-609913 (**2b**·6THF), CCDC-609911 (**4**·THF), CCDC-609912 (**5**·10THF), and CCDC-609914 (**6**·2THF) contain the supplementary crystallographic data for this paper. These data can be obtained free of charge from the Cambridge Crystallographic Data Centre via www.ccdc.cam.ac.uk/data_request/cif.

(22) Sheldrick, G. M. *SADABS—A Program for Empirical Absorption Correction*; Universität Göttingen: Göttingen, Germany, 1998.

(23) Farrugia, L. J. *J. Appl. Crystallogr.* **1999**, *32*, 837.

(24) Sheldrick, G. M. *SHELXS97, SHELXL97—Programs for Crystal Structure Analysis*, release 97-2; Universität Göttingen: Göttingen, Germany, 1998.

Table 1. Crystallographic Data for **2b**·6THF, **4**·THF, **5**·10THF, and **6**·2THF

compound	2b ·6THF	4 ·THF	5 ·10THF	6 ·2THF
empirical formula	C ₁₁₀ H ₁₁₈ O ₁₀ P ₄ Rh ₂ S ₂	C ₄₅ H ₄₆ O ₃ P ₃ RhS	C ₁₉₀ H ₁₉₈ O ₂₂ P ₆ Rh ₄ S ₆	C ₆₀ H ₉₄ O ₁₀ P ₄ Rh ₂ S ₄
mol wt	1993.86	862.70	3623.30	1433.29
<i>T</i> [K]	207(2)	213(2)	180(2)	213(2)
λ [pm]	71.073	71.073	71.073	71.073
cryst syst	monoclinic	monoclinic	triclinic	monoclinic
space group	<i>P</i> 2 ₁ / <i>n</i>	<i>C</i> 2/ <i>c</i>	<i>P</i> $\bar{1}$	<i>P</i> 2 ₁ / <i>n</i>
<i>a</i> [pm]	1846.2(3)	3626.5(2)	1496.0(1)	1566.4(1)
<i>b</i> [pm]	2613.8(3)	1256.85(7)	1911.4(1)	1066.50(7)
<i>c</i> [pm]	2170.4(3)	2022.6(1)	2051.8(2)	2040.7(2)
α [deg]	90	90	113.635(5)	90
β [deg]	102.46(2)	115.048(2)	106.230(6)	96.08(1)
γ [deg]	90	90	94.296(6)	90
<i>V</i> [nm ³]	10.23(1)	8.3516(8)	5.0427(6)	3.3900(5)
<i>Z</i>	4	8	1	2
ρ_{calcd} [g·cm ⁻³]	1.295	1.372	1.193	1.404
μ [mm ⁻¹]	0.483	0.613	0.489	0.756
<i>F</i> (000)	4160	3568	1880	1496
cryst size [mm]	0.40 × 0.30 × 0.25	0.60 × 0.40 × 0.20	0.40 × 0.20 × 0.20	0.45 × 0.20 × 0.05
Θ range [deg]	2.04–26.04	1.91–28.29	3.11–23.25	2.01–25.92
<i>h</i> , <i>k</i> , <i>l</i> collected	–22 ≤ <i>h</i> ≤ 22 –32 ≤ <i>k</i> ≤ 32 –24 ≤ <i>l</i> ≤ 26	–48 ≤ <i>h</i> ≤ 47 –16 ≤ <i>k</i> ≤ 16 –26 ≤ <i>l</i> ≤ 26	–16 ≤ <i>h</i> ≤ 16 –20 ≤ <i>k</i> ≤ 21 –22 ≤ <i>l</i> ≤ 22	–19 ≤ <i>h</i> ≤ 19 –11 ≤ <i>k</i> ≤ 12 –24 ≤ <i>l</i> ≤ 24
reflns measd	68 058	37 002	47 746	20 733
unique reflns	19 707	9971	14 452	6466
restraints/params	150/1005	47/530	1106/1178	10/368
GOF (all data)	0.881	1.030	0.928	0.704
final <i>R</i> indices [<i>I</i> > 2 σ (<i>I</i>)]	<i>R</i> 1 = 0.0429 w <i>R</i> 2 = 0.1139	<i>R</i> 1 = 0.0279 w <i>R</i> 2 = 0.0701	<i>R</i> 1 = 0.0776 w <i>R</i> 2 = 0.2057	<i>R</i> 1 = 0.0346 w <i>R</i> 2 = 0.0732
<i>R</i> indices	<i>R</i> 1 = 0.0645	<i>R</i> 1 = 0.0439	<i>R</i> 1 = 0.1299	<i>R</i> 1 = 0.0758
all data	w <i>R</i> 2 = 0.1192	w <i>R</i> 2 = 0.0751	w <i>R</i> 2 = 0.2305	w <i>R</i> 2 = 0.0776
$\Delta\rho$ (max/min) [<i>e</i> ·Å ⁻³]	1.367/–0.514	0.788/–0.418	1.217/–0.650	0.571/–0.312

Discussion

Because of the pronounced tendency of rhodium(I) complexes to undergo oxidative addition, salt elimination was preferred over base-mediated HCl elimination for the synthesis of the rhodium(I) thiolato complexes. For this purpose, the potassium salt of H₂mba was prepared by deprotonation with 1 equiv of KO^tBu. The resulting product, K(Hmba) (**1**), is a colorless solid. As the p*K*_a values of benzoic acid and thiophenol in nonprotic solvents are very similar (e.g., 11.1^{25a} and 10.3^{25b} in DMSO, respectively), it was impossible to predict the deprotonation site. Unfortunately, the spectroscopic data of K(Hmba) (**1**) are not unambiguous. Thus, in the ¹H NMR spectrum (in DMSO), a signal at 11.6 ppm seems to indicate the presence of the protonated carboxyl group in solution, while the IR spectrum of solid **1** seems to indicate deprotonation of the carboxyl group, as the typical absorptions for the asymmetric and symmetric stretching vibrations of a COO group in carboxylates are observed at 1542 and 1400 cm⁻¹, respectively, while the C=O vibration of the starting material H₂mba (1678 cm⁻¹) is no longer observed. However, different structures in the solid state and in solution cannot be excluded.

Syntheses of the Rhodium(I) Complexes. The reaction of K(Hmba) (**1**) with 1 equiv of [RhCl(PPh₃)₃] yields exclusively the dimer [{Rh(μ -SC₆H₄COOH)(PPh₃)₂}]₂ (**2b**), which forms with the elimination of one phosphane ligand per rhodium atom. To achieve full conversion of the starting

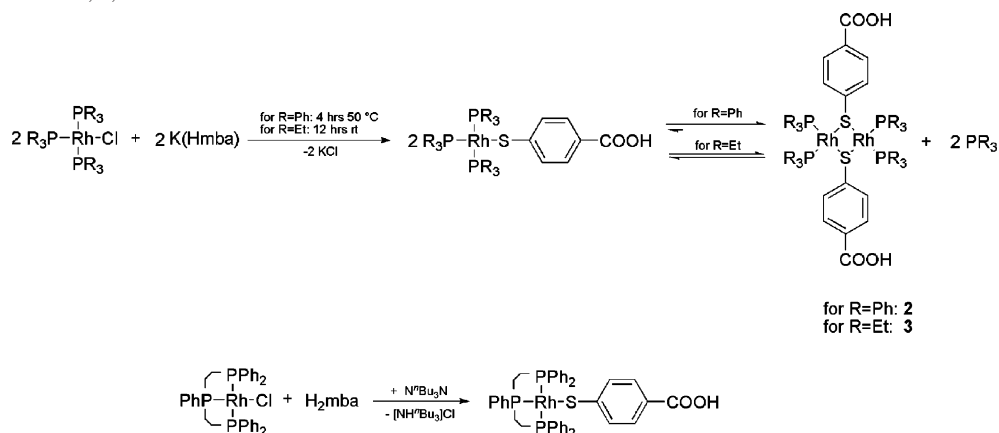
material, heating to 50 °C for 4 h is necessary. Very small amounts of the monomer [Rh(SC₆H₄COOH)(PPh₃)₃] are observed in the ³¹P NMR spectrum of highly concentrated solutions of **2b** when a large excess of PPh₃ (15-fold) is present (Scheme 2).

To prevent dimerization, two strategies were employed: (1) utilization of the electron-richer triethylphosphane and (2) exploitation of the chelate effect by using PPh(C₂H₄PPh₂)₂ as a coligand. The reaction of K(Hmba) with [RhCl(PET₃)₃] (1:1) proceeds at room temperature and yields a mixture of the monomeric and dimeric rhodium(I) complexes. The equilibrium is fully shifted toward the monomer [Rh(SC₆H₄COOH)(PET₃)₃] (**3a**) when an excess of PET₃ is present. No dimeric complex is formed when PPh(C₂H₄PPh₂)₂ is used, [Rh(SC₆H₄COOH){PPh(C₂H₄PPh₂)₂}] (**4**) being the only product. Because of the low solubility of **4**, separation from KCl proved difficult. Therefore, base-mediated HCl elimination with NⁿBu₃ was the preferred synthetic approach here, as the ammonium salt [NHⁿBu₃]Cl is soluble in toluene and can thus be easily removed (Scheme 2).

The composition of the rhodium(I) complexes was verified by elemental analysis and mass spectrometry. FAB mass spectrometry proved to be suitable for investigating **2b** and **4**, while the investigation of **3a** was rather difficult. Neither ionization with electron impact, electrospray ionization, or matrix-assisted laser desorption ionization nor that with laser desorption ionization resulted in informative spectra. In the FAB mass spectrum, only three fragments of very low intensity could be identified, [M + H – 18]⁺ (cleavage of H₂O), [M + H – 44]⁺ (cleavage of CO₂), and [M + H – 46]⁺ (cleavage of formic acid or CO and H₂O, respectively).

(25) (a) Piljugin, V. S.; Kusnetzova, S. L.; Schkunova, N. A. *Zh. Obshch. Khim.* **1986**, *56*, 425. (b) Bordwell, F. G.; Cheung, J.-P.; Ji, G.-Z.; Satish, A. V.; Zhang, X. *J. Am. Chem. Soc.* **1991**, *113*, 9790.

Scheme 2. Syntheses of 2, 3, and 4



Solid-State Structures of the Rhodium(I) Complexes.

X-ray structure determinations were carried out on single crystals of **2b** and **4**. $[\{\text{Rh}(\mu\text{-SC}_6\text{H}_4\text{COOH})(\text{PPh}_3)_2\}_2]$ (**2b**) crystallizes in the monoclinic space group $P2_1/n$ with one molecule per asymmetric unit and six molecules of THF per molecule of **2b**. The central structural motif is a puckered Rh_2S_2 ring (dihedral angle $\text{Rh1-S1-S2/Rh2-S1-S2} = 139^\circ$). With the exception of $[\{\text{Rh}(\mu\text{-SC}_6\text{H}_5)(\text{dippe})_2\}_2]$ (*dippe* = $i\text{-Pr}_2\text{PCH}_2\text{CH}_2\text{P}i\text{-Pr}_2$),²⁶ which exhibits a planar Rh_2S_2 ring, all other structurally characterized complexes of the type $[\{\text{Rh}(\mu\text{-SR})(\text{PR}_3)_2\}_2]$ show a puckered ring. The preference for the bent structure despite a small energy difference, as shown by theoretical calculations,²⁷ is explained by the pronounced tendency of sulfur to undergo sp^3 hybridization and of rhodium to form d^8-d^8 contacts. In **2b**, each rhodium atom is coordinated in a distorted square-planar fashion by two phosphane and two bridging thiolato ligands (Figure 1). The sum of bond angles at S1 and S2 are 304.23 and 305.90° , respectively, and the $\text{Rh1}\cdots\text{Rh2}$ distance is 338 pm (Table 2).

For **2b**, the syn-exo conformer is present in the solid state, which is stabilized by $\pi-\pi$ stacking of the aromatic rings of the 4-carboxyphenylthiolato ligands (average distance

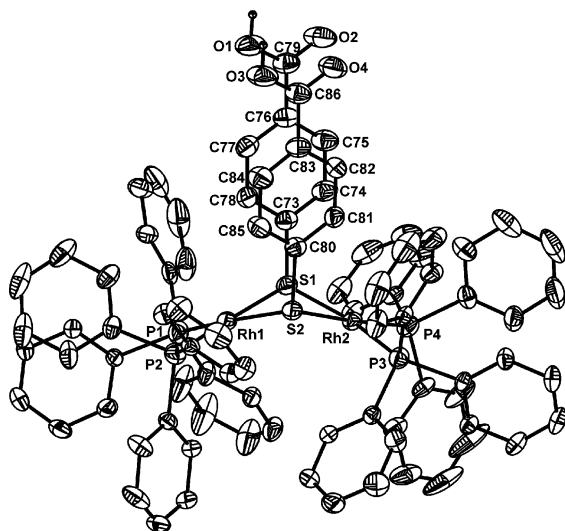


Figure 1. View of the molecular structure of $[\{\text{Rh}(\mu\text{-SC}_6\text{H}_4\text{COOH})(\text{PPh}_3)_2\}_2]$ (**2b**). Hydrogen atoms (other than H10 and H30) and solvent molecules have been omitted for clarity. Thermal ellipsoid level: 30%.

Table 2. Selected Bond Lengths [pm] and Angles [deg] for **2b**·6THF and **4**·THF

	2b ·6 THF		4 ·THF
Rh1–S1	239.27(4)	Rh1–S1	240.61(5)
Rh2–S1	240.35(3)	Rh1–P1	228.78(6)
Rh1–P1	226.82(2)	Rh1–P2	219.02(5)
Rh2–P3	225.06(2)	Rh1–P3	228.42(6)
Rh1–P2	223.59(3)	C41–O1	124.7(3)
Rh2–P4	226.09(3)	C41–O2	130.6(3)
Rh1–S2	237.78(3)	O1–H10	82.02(2)
Rh2–S2	239.02(2)	S1–Rh1–P1	97.14(2)
S1–Rh1–S2	82.223(7)	P1–Rh1–P2	83.65(2)
P1–Rh1–P2	97.762(7)	P2–Rh1–P3	83.81(2)
S1–Rh1–P1	86.72(3)	P3–Rh1–S1	95.15(2)
S2–Rh1–P2	93.27(3)	P1–Rh1–P3	159.19(2)
S1–Rh2–S2	81.739(7)	S1–Rh1–P2	178.73(2)
P3–Rh2–P4	97.550(7)	C38–C41–O1	120.9(2)
S2–Rh2–P3	176.35(4)	C38–C41–O2	116.0(2)
S1–Rh2–P4	166.32(3)	O1–C41–O2	123.1(2)
S1–Rh2–S2	81.739(7)	C41–O1–H10	123.7(4)

between two neighboring carbon atoms is 358 pm; the longest distance is 375 pm), in which the aromatic rings of the Hmba ligands exhibit a “face-to-face” arrangement.²⁸ Hydrogen bonds between the carboxyl groups of two of these molecules result in a centrosymmetric tetranuclear unit which is located on a crystallographic inversion center (Figure 2). Accordingly, in the IR spectrum, **2b** exhibits the $\text{C}=\text{O}$ vibration at 1682 cm^{-1} and the “out-of-plane” deformation $\delta_{(-\text{OH}\cdots\text{O})}$ at 913 cm^{-1} , as expected for hydrogen-bonded dimers.²⁹

$[\text{Rh}(\text{SC}_6\text{H}_4\text{COOH})\{\text{PPh}(\text{C}_2\text{H}_4\text{PPh}_2)_2\}]$ (**4**) crystallizes in the monoclinic space group $C2/c$ with one molecule of **4** and one highly disordered THF molecule in the asymmetric unit cell. The rhodium atom is coordinated in a distorted square-planar fashion by the three phosphorus atoms of the triphos ligand and a terminal thiolato ligand (Figure 3 and Table 2). The P1-Rh1-P2 and P2-Rh1-P3 bond angles deviate from 90° by 6° and P1-Rh1-P3 from 180° by 21° , which shows the strain in the Rh-P-C-C-P five-membered rings. As was observed for **2b**, two molecules of

(26) Oster, S. S.; Jones, W. D. *Inorg. Chim. Acta* **2004**, *357*, 1836.

(27) Aullón, G.; Ujaque, G.; Lledós, A.; Alvarez, S. *Chem.—Eur. J.* **1999**, *5*, 1391.

(28) Roesky, H. W.; Andruh, M. *Coord. Chem. Rev.* **2003**, *236*, 91.

(29) Günzler, H.; Gremlich, H.-U. In *IR Spectroscopy: An Introduction*; Wiley-VCH: New York, 2002.

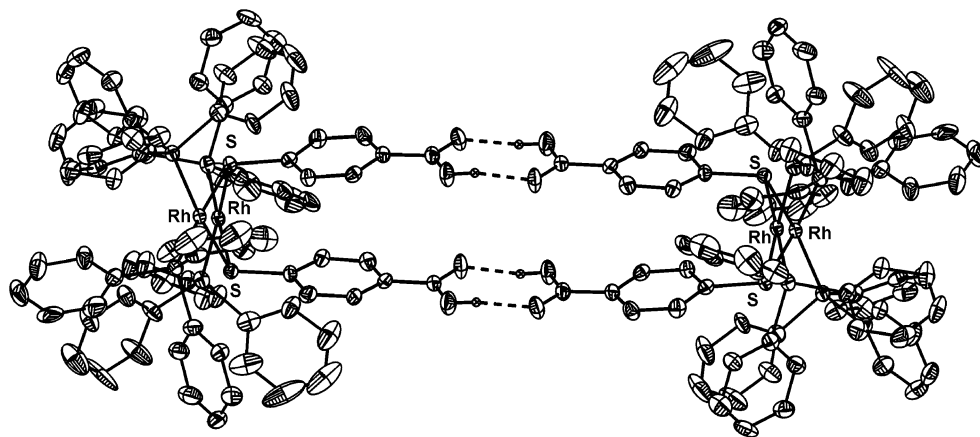


Figure 2. Association of **2b** in the solid state. Thermal ellipsoid level: 30%.

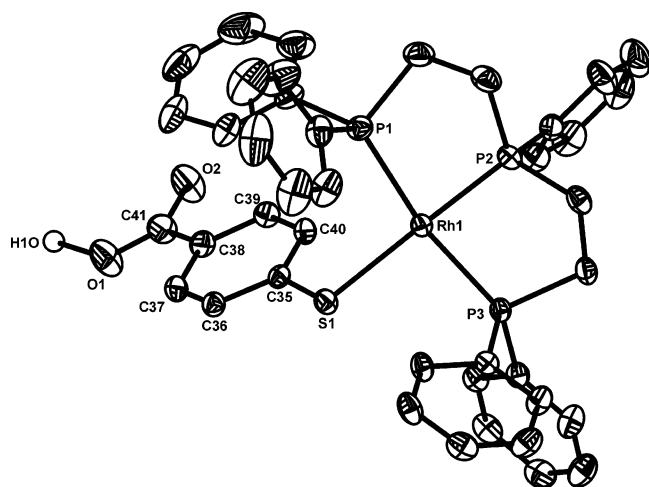


Figure 3. View of the molecular structure of $[\text{Rh}(\text{SC}_6\text{H}_4\text{COOH})\{\text{PPh}(\text{C}_2\text{H}_4\text{PPh}_2)_2\}]$ (**4**). Hydrogen atoms (other than H1O) and solvent molecules have been omitted for clarity. Thermal ellipsoid level: 30%.

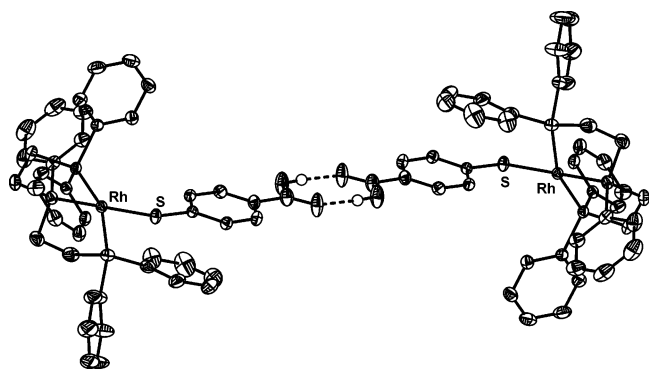


Figure 4. Association of **4** in the solid state.

4 dimerize via hydrogen bonds and the dimer is located on a crystallographic inversion center (Figure 4).

No single crystals could be obtained of **3a**, probably because of the monomer–dimer equilibrium. If a THF solution of **3a** is treated with toluene or *n*-hexane, or if the synthesis is performed in a THF/toluene mixture, a red solid precipitates which is insoluble in common organic solvents (*n*-hexane, toluene, THF, acetonitrile, DMF, and DMSO). The solid-state $^{31}\text{P}\{^1\text{H}\}$ NMR spectrum of this solid shows two signals at 20 and 75 ppm, in a ratio of 2:1, indicating three phosphorus nuclei, of which two are magnetically

equivalent, as expected for **3a**. However, in the IR spectrum of the insoluble solid, the C=O vibration is observed at 1682 cm^{-1} (H_2mba : $\tilde{\nu}_{\text{CO}} = 1678\text{ cm}^{-1}$), while for **3a**, this appears at 1663 cm^{-1} . This indicates that different modes of association of the carboxyl groups are possible in the solid state and apparently result in different solubility.

Structures in Solution. **2b** undergoes dissociation of PPh_3 in solution and exists in equilibrium with unknown species which show a very broad signal at 40 ppm in the $^{31}\text{P}\{^1\text{H}\}$ NMR spectrum. As could be shown by exchange experiments with $\text{PPh}_2(p\text{-tolyl})$, the free phosphane ligands exchange with the coordinated ones, indicating fluxional behavior in solution. However, **2b** is stable when an excess of 1 equiv of PPh_3 is present and shows a doublet at 41.9 ppm ($^1J_{\text{PRh}} = 168.9\text{ Hz}$) in the $^{31}\text{P}\{^1\text{H}\}$ NMR spectrum. As in similar compounds,^{8–10} no $^3J_{\text{PRh}}$ coupling is observed; that is, it is clearly smaller than the line width of the signals (9 Hz).

In solution, complexes of general formula $[\{\text{Rh}(\mu\text{-SR})\text{-}(\text{PR}'_3)_2\}_2]$ with a puckered Rh_2S_2 ring can exist as different stereoisomers, in which the thiolates occupy different positions, that is, the syn or anti conformation. In the syn arrangement, the thiolates can occupy the exo or endo position³⁰ (Figure 5).

Variable-temperature $^{31}\text{P}\{^1\text{H}\}$ NMR spectroscopic investigations in $\text{THF-}d_8$ showed splitting of the signal for **2b** into two broad signals below 185 K. Unfortunately, no resolution of the fine splitting could be achieved because of solvent restrictions. Theoretical calculations³¹ and experimental studies on $[\{\text{Rh}(\mu\text{-SR})(\text{dippe})\}_2]$ ($\text{dippe} = {}^i\text{Pr}_2\text{PCH}_2\text{-CH}_2\text{P}^i\text{Pr}_2$; R = H, Me, Cy, *o*-biphenyl, Ph)³⁰ showed that the conversion from the syn to the anti isomer (inversion at the sulfur center) has a higher free reaction enthalpy (ca. 40 kJ/mol) than ring inversion between the exo and endo forms (<35 kJ/mol). Therefore, it seems likely that the two signals can be assigned to the syn and anti isomers.

For the monomer of **3a** and for **4**, a doublet of doublets and a doublet of triplets are observed in the $^{31}\text{P}\{^1\text{H}\}$ NMR spectrum. Phosphorus–rhodium coupling constants of 136.4

(30) Oster, S. S.; Jones, W. D. *Inorg. Chim. Acta* **2004**, *357*, 1836.

(31) Duran, N.; González-Duarte, P.; Lledós, A.; Parella, T.; Sola, J.; Ujaque, G.; Clegg, W.; Fraser, K. A. *Inorg. Chim. Acta* **1997**, *265*, 89.

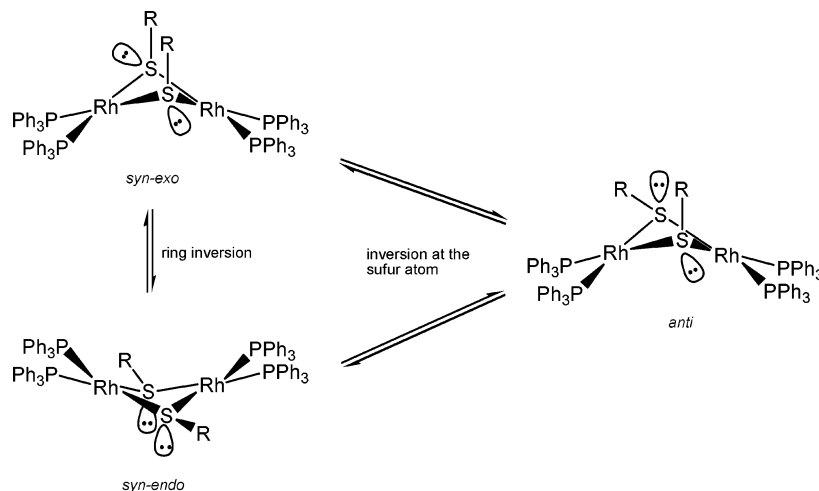


Figure 5. Equilibrium between the different conformers in a solution of **2b**.

Hz (P trans to thiolate) and 161.8 Hz (2P cis to thiolate) for **3a** and 138.2 Hz (P trans to thiolate) and 150.9 Hz (2P cis to thiolate) for **4** are typical for rhodium(I) complexes.³² While no dissociation of a phosphane ligand is observed for **4**, for **3a**, a singlet for free PEt_3 and a doublet for the dimeric form are observed, as was also found for **2b**. With an excess of PEt_3 , the equilibrium can be shifted to the monomeric form (Scheme 2).

After purification, **4** is insoluble in common organic solvents (*n*-hexane, toluene, THF, acetonitrile, and DMSO) and dissolves in DMF with decomposition. Low solubility was also observed for the starting material, $[\text{RhCl}\{\text{PPh}(\text{C}_2\text{H}_4\text{-PPh}_2)_2\}]$, for which bridging bonding modes of the tripodal phosphane ligand were suggested to account for this unexpected behavior.^{21a} However, X-ray analysis later showed this complex to be monomeric in the solid state;^{21b} thus, there is still no rational explanation for the low solubility. Therefore, NMR spectroscopic characterization of **4** was carried out on the slightly impure, but still soluble, compound, and no ^{13}C NMR spectroscopic characterization was performed. In the ^1H NMR spectrum, the signals for the AA'BB' spin system for the aromatic ring of the 4-thiolato-benzoate ligand in **2–4** were broader than the other signals; this indicates hindered rotation of the $\text{SC}_6\text{H}_4\text{COOH}$ group, which prevents simulation of the spectra to determine the coupling constants.

Reactivity of the Rhodium(I) Complexes. Interesting insight into the reactivity of the rhodium(I) complexes **2b** and **3a** is given by two compounds which were isolated during the experiments, $[\{\text{Rh}^{\text{I}}\text{Rh}^{\text{III}}(\mu\text{-SC}_6\text{H}_4\text{COO})(\mu\text{-SC}_6\text{H}_4\text{COOH})(\text{SC}_6\text{H}_4\text{COOH})(\text{PPh}_3)_3\}_2]$ (**5**) and $[\{\text{Rh}(\mu\text{-SC}_6\text{H}_4\text{COO})(\text{SC}_6\text{H}_4\text{COOH})(\text{PEt}_3)_2\}_2]$ (**6**), and, because of low solubility and low yield (a few crystals), were only characterized by X-ray crystallography.

The dimeric rhodium(III) complex $[\{\text{Rh}(\mu\text{-SC}_6\text{H}_4\text{COO})(\text{SC}_6\text{H}_4\text{COOH})(\text{PEt}_3)_2\}_2]$ (**6**) (Figure 6, top) was isolated as a side product in the synthesis of **3a** and crystallized on the vapor diffusion of diethyl ether into a concentrated solution of the reaction mixture. Compound **6** might have been

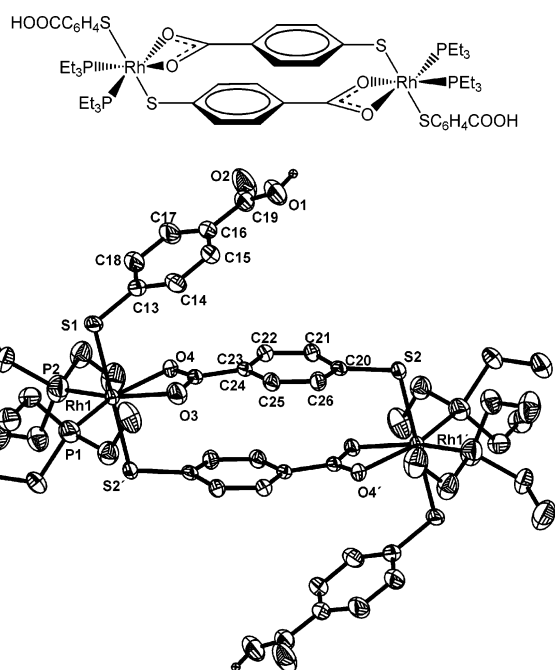


Figure 6. View of the molecular structure of $[\{\text{Rh}(\mu\text{-SC}_6\text{H}_4\text{COO})(\text{SC}_6\text{H}_4\text{COOH})(\text{PEt}_3)_2\}_2]$ (**6**). Hydrogen atoms (other than H1) and solvent molecules have been omitted for clarity. Thermal ellipsoid level: 30%.

formed via the oxidative addition of additional $\text{K}(\text{Hmba})$, a reaction already known for other rhodium(I) complexes,^{7a} which is employed in slight excess in the reaction to facilitate the full conversion of $[\text{RhCl}(\text{PEt}_3)_3]$. The spectrum of the reaction solution showed the additional signal for **6** at 34.9 ppm with a Rh–P coupling constant of 123.9 Hz, which is typical for rhodium(III) complexes. The same spectrum is observed when 1 equiv of $\text{K}(\text{Hmba})$ is added to a THF solution of **3** at room temperature. Unfortunately, isolation of pure **6** from this reaction fails because of the low solubility of **6** in common organic solvents. A better solubility would be necessary to separate it from residual $\text{K}(\text{Hmba})$.

When a solution of **2b** in THF was layered with *n*-hexane to obtain single crystals, the color of the solution surprisingly changed from deep orange to brown, and dark brown crystals of the mixed-valent complex $[\{\text{Rh}^{\text{I}}\text{Rh}^{\text{III}}(\mu\text{-SC}_6\text{H}_4\text{COO})(\mu\text{-SC}_6\text{H}_4\text{COOH})(\text{SC}_6\text{H}_4\text{COOH})(\text{PPh}_3)_3\}_2]$ (**5**) (Figure 7, top)

(32) Brown, T. H.; Green, P. J. *J. Am. Chem. Soc.* **1970**, *92*, 2359.

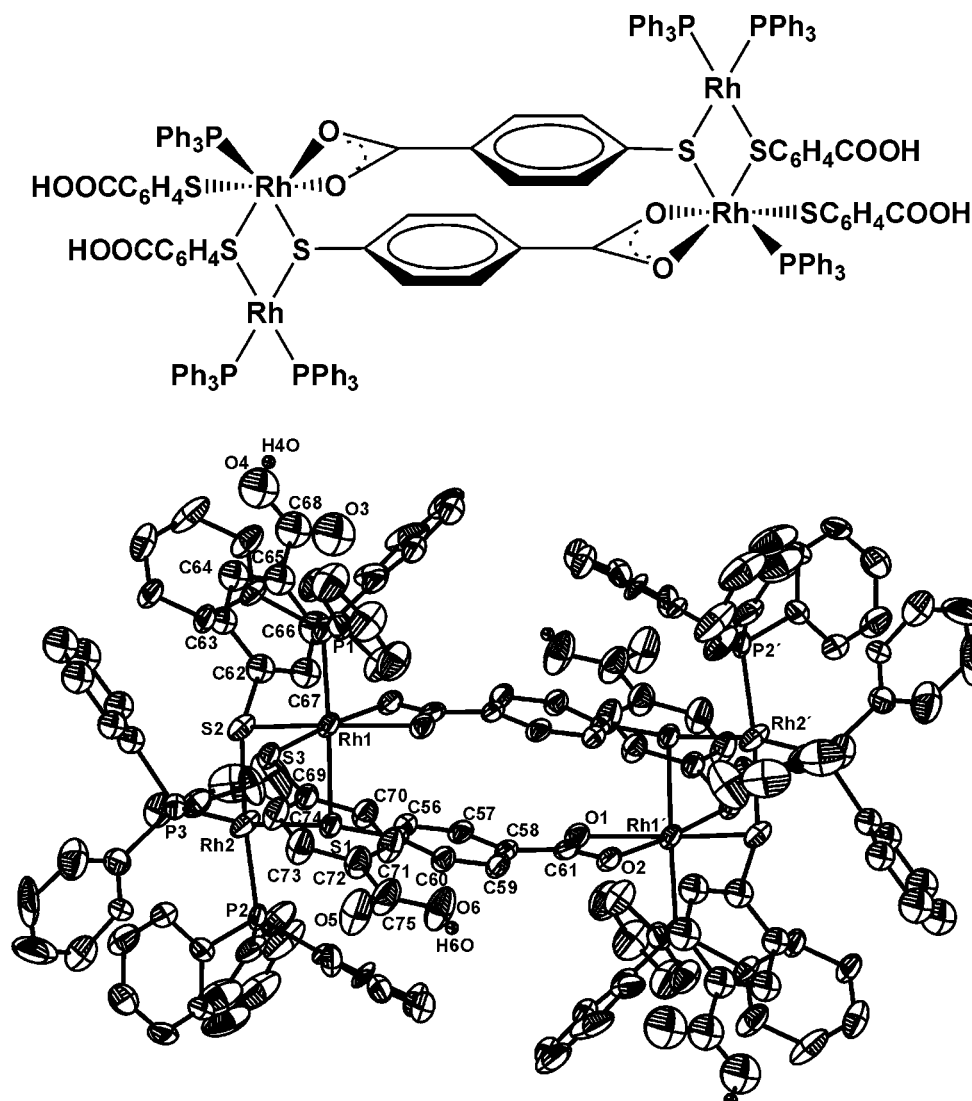


Figure 7. Schematic drawing (top) and view of the molecular structure (bottom) of $[\{\text{Rh}^{\text{I}}\text{Rh}^{\text{III}}(\mu\text{-SC}_6\text{H}_4\text{COO})(\mu\text{-SC}_6\text{H}_4\text{COOH})(\text{SC}_6\text{H}_4\text{COOH})(\text{PPh}_3)_3\}_2]$ (**5**). Hydrogen atoms (other than H4O and H6O) and solvent molecules have been omitted for clarity. Thermal ellipsoid level: 30%.

formed besides a brown insoluble precipitate. The mechanism for the formation of **5** is less straightforward, because there is no excess $\text{K}(\text{Hmba})$ present in solution. As mentioned above, **2b** eliminates PPh_3 with the formation of unknown species in solution. Therefore, the removal of free PPh_3 by the addition of *n*-hexane (PPh_3 is not very soluble in *n*-hexane) could result in the decomposition of **2b**. The formation of an insoluble brown precipitate, which does not show any $\text{C}=\text{O}$ vibration in the IR spectrum, besides **5** indicates that the decomposition takes place with cleavage of the rhodium–thiolate bond, and thus, 4-thiolatobenzoic acid is present as a monoanion or neutral thiol, which can oxidatively add to residual **2b** to yield **5**. All known mixed-valent rhodium(I)–rhodium(III) complexes were synthesized by the selective oxidative addition of one rhodium center in dinuclear rhodium(I) complexes.³³

Because of solvent loss during the preparation of single crystals of **5** for X-ray measurement, the quality of the data is rather low and only a structural motif was obtained. Compound **5** crystallizes in the triclinic space group $P\bar{1}$ with one half molecule of **5** (Figure 7, Table 3) in the asymmetric

Table 3. Selected Bond Lengths [pm] and Angles [deg] for **5**·10THF and **6**·2THF

5·10THF		6·2THF	
Rh1–O1	221.2(5)	Rh1–O3	219.4(3)
Rh1–O2	211.4(5)	Rh1–O4	218.4(3)
Rh1–P1	233.2(2)	Rh1–P1	226.7(1)
Rh1–S1	239.1(2)	Rh1–P2	226.0(1)
Rh1–S2	231.6(2)	Rh1–O3	219.4(3)
Rh1–S3	232.4(2)	Rh1–S1	240.0(1)
Rh2–S1	237.7(2)	Rh1–S2	239.6(1)
Rh2–S2	236.0(2)	O3–Rh1–O4	60.4(1)
Rh2–P2	219(2)	O3–Rh1–P1	100.46(8)
Rh2–P3	224.1(5)	O4–Rh1–P2	101.70(9)
S1–Rh1–P1	173.79(8)	S1–Rh1–S2	178.99(5)
S2–Rh1–S3	81.40(8)		
O1–Rh1–O2	60.8(2)		
S2–Rh1–O2	103.7(2)		
S3–Rh1–O1	113.7(2)		
S1–Rh2–S2	81.87(8)		
S2–Rh2–P3	91.7(1)		
S1–Rh2–P2	86.7(5)		
P2–Rh2–P3	100.9(5)		

unit and 10 THF molecules per unit cell. Some of the phenyl rings and the bridging ligands are highly disordered. The

central Rh₂S₂ ring as the structural motif of **2b** still exists, but one of the rhodium centers, rhodium(III) (Rh^{III}), is now coordinated octahedrally by two thiolates and one S-coordinated thiolatobenzoato ligand (mba²⁻) in a facial geometry, one bidentate carboxylato group, and one phosphane ligand. The rhodium(I) group, Rh(PPh₃)₂ (Rh^I), and rhodium(III) are bridged by one of the three thiolato ligands and the S-coordinated thiolatobenzoato ligand. Rh^I has a distorted square-planar environment. The Rh₂S₂ ring is nearly planar (dihedral angle Rh^I–S1–S2/Rh^{III}–S1–S2 = 174.1°). The deviation from planarity is possibly due to packing effects. Two dimeric Rh^I–Rh^{III} units are bridged by two mba²⁻ dianions to give a centrosymmetric tetranuclear complex. As in **2b**, “π–π stacking” stabilizes the molecule, but geometry restraints force the two aromatic rings into an “offset” or “slipped” arrangement. The distance of the *ipso*-carbon atom C58 to the plane of the opposite aromatic ring (C55′–C60′) is 331 pm.²⁸ In the solid state, **5** forms one-dimensional zigzag chains via hydrogen bonds of the free carboxyl groups of the terminal thiolato ligands (S3, C75, O5, and O6, see Figure 1 in the Supporting Information).

[{Rh(μ-SC₆H₄COO)(SC₆H₄COOH)(PEt₃)₂}₂] (**6**) crystallizes in the monoclinic space group *P*2₁/*n* with one half molecule of **6** in the asymmetric unit and four molecules of THF in the unit cell. Like **5**, **6** has a 16-membered Rh^{III}₂(SC₆H₄COO)₂ ring, which is located on a crystallographic inversion center, as the central motif (Figure 6,

- (33) (a) Tejel, C.; Ciriano, M. A.; Edwards, A. J.; Lahoz, F. J.; Oro, L. A. *Organometallics* **1997**, *16*, 45. (b) Tejel, C.; Ciriano, M. A.; Edwards, A. J.; Lahoz, F. J.; Oro, L. A. *Organometallics* **2000**, *19*, 4968. (c) Pinillos, M. T.; Elduque, A.; Oro, L. A. *Polyhedron* **1992**, *11*, 1007. (d) Ho, D. G.; Ismail, R.; Franco, N.; Gao, R.; Leverich, E. P.; Tsyba, I.; Ho, N. N.; Bau, R.; Selke, M. *Chem. Commun.* **2002**, 570.

Table 3), but in contrast to **5**, there is no additional four-membered Rh₂S₂ ring. The rhodium(III) center is coordinated octahedrally by two phosphane ligands in *cis* positions, two thiolato ligands in *trans* positions, and one bidentate carboxylato group of the bridging 4-thiolatobenzoato ligand (mba²⁻). As in **5**, the free carboxyl groups associate via hydrogen bonds to give zigzag chains of **6** (see Figure 2 in the Supporting Information).

Conclusion

Variation of the phosphane ligands L in rhodium(I) complexes of the type [Rh(SC₆H₄COOH)L] influences their tendency to dimerize with the dissociation of phosphane. For L = (PPh₃)₃, mainly the dimer is observed. An equilibrium between the monomeric and dimeric form is observed for the electron-rich triethylphosphane [L = (PEt₃)₃], which is shifted to the monomer by excess free PEt₃ in solution. The chelate effect of the PPh(C₂H₄PPh₂)₂ ligand completely inhibits dissociation and stabilizes the monomeric form. As was shown by the isolation and structural characterization of a side product and a decomposition product, the rhodium(I) complexes are susceptible to the oxidative addition of (Hmba) to form rhodium(III) complexes.

Acknowledgment. U.H. thanks the Studienstiftung des Deutschen Volkes for a Ph. D. grant. Financial support from the Graduiertenkolleg 378 and a generous donation of RhCl₃ from Umicore AG & Co KG are gratefully acknowledged.

Supporting Information Available: Figures of the associations of **5** and **6** in the solid state. This material is available free of charge via the Internet at <http://pubs.acs.org>.

IC0610684